Supporting Information

A Rhodamine/BODIPY-Based Fluorescent Probe for the Differential Detection of Hg(II) and Au(III)†

Erman Karakuş‡, Muhammed Üçüncü‡ and Mustafa Emrullahoğlu*[a]

Department of Chemistry, Faculty of Science, İzmir Institute of Technology, Urla, 35430, Izmir, Turkey

‡ These authors contributed equally to this work
† Dedicated to the memory of Prof.Dr. Ayhan S. Demir (1950-2012)

CONTENTS **PAGE**

1. General Methods: All reagents were purchased from commercial suppliers (Aldrich and Merck) and used without further purification. ^{1}H NMR and ^{13}C NMR were measured on a Varian VNMRJ 400 Nuclear Magnetic Resonance Spectrometer. Bruker MALDI-TOF-TOF Mass Spectrometer was used for mass spectrometry analysis. UV absorption spectra were obtained on Shimadzu UV-2550 Spectrophotometer. Fluorescence emission spectra were obtained using Varian Cary Eclipse Fluorescence spectrophotometer. Cell imaging was performed with Olympus CKX41 fluorescence microscope. Samples were contained in 10.0 mm path length quartz cuvettes (2.0 mL volume). Upon excitation at 470 nm, the emission spectra were integrated over the range 480 nm to 700 nm for Au^{3+} measurements. Upon excitation at 525 nm, the emission spectra were integrated over the range 535 nm to 700 nm for Hg^{2+} measurements. The pH was recorded by HI-8014 instrument (HANNA). All measurements were conducted at least in triplicate.

2. Synthesis Section

Synthesis of RhS-BOD

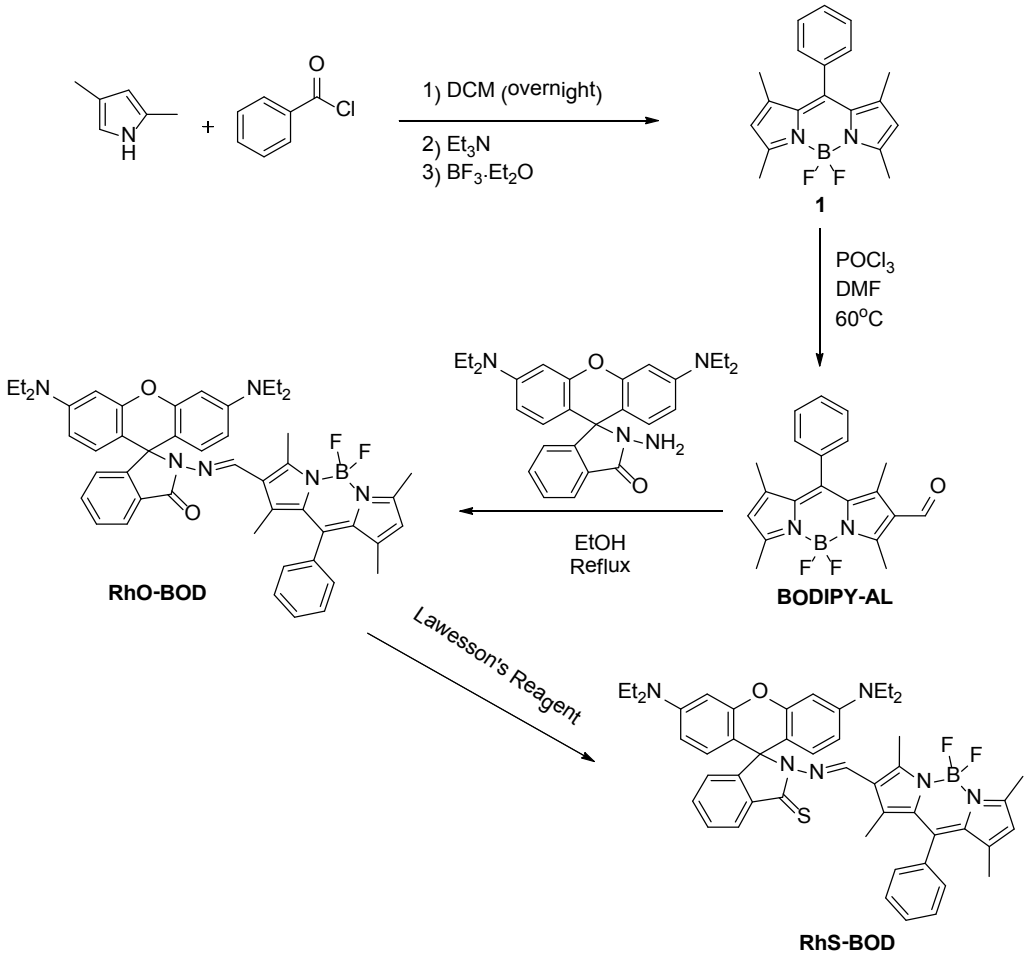

Scheme S1 Synthesis route of R**hS-BOD**

Compound **1** was synthesized according to known procedure.[1] Formylation reaction of compound **1** was performed by using known (Vilsmeier Haack reaction) procedure.[2] To a solution of rhodamine B (150mg, 0.33 mmol) in absolute ethanol (10 ml) was added **BODIPY-AL** (116mg, 0.33mmol) and the solution was stirred overnight at reflux temperature.[3] The reaction mixture was extracted with dichloromethane (3 x 10 mL). Then, the collected organic layers were dried over anhydrous $MgSO_4$, concentrated under vacuum, and purified by column chromatography (hexane/EtOAc = 8/1) to give 156 mg of **RhO-BOD** (60%) as a pink oil. ^{1}H-NMR (400 MHz, $CDCl_3$) δ: 9.12 (s, 1H), 7.94-7.92 (m, 1H), 7.49-7.45 (m, 4H), 7.20-7.12 (m, 3H), 6.98 (t, J=7.2 Hz, 1H), 6.47-6.26 (m, 6H), 5.99 (s, 1H), 3.32 (br. s, 8H), 2.47 (s, 3H), 2.31 (s, 3H), 1.33 (s, 6H), 1.15 (br. s, 12H). ^{13}C NMR (100 MHz, $CDCl_3$) δ: 164.13, 156.58, 153.37, 150.80, 148.80, 143.88, 142.01, 140.88, 137.76, 134.76, 132.06, 131.99, 130.92, 130.61, 129.88, 129.18, 128.28, 127.89, 126.00, 124.04, 123.06, 121.89, 107.88, 106.28, 97.75, 66.23, 44.36, 14.68, 14.47, 14.16, 12.58, 11.99. MS (MALDI-TOF): m/z: Calcd. for $C_{48}H_{49}BF_2N_6O_2$: 791.479 $[M+H]^+$, Found: 791.471 $[M+H]^+$. The **RhO-BOD** (100 mg, 0.13mmol) and Lawesson's reagent (53mg, 0.13mmol) were dissolved in dry toluene, and reaction mixture was refluxed for 2 h under N_2 atmosphere. After removal of toluene, the residue was purified by column chromatography (hexane/EtOAc = 10/1) to give 42 mg of **RhS-BOD** (40%) as a purple solid. ^{1}H-NMR (400 MHz, $CDCl_3$) δ: 8.63 (s, 1H), 8.07 (dd, J=6.0 Hz, 3.2 Hz, 1H), 7.48-7.47 (m, 3H), 7.39 (dd, J=6.0 Hz, 3.2 Hz, 2H), 7.27-7.26 (m, 2H), 7.10 (dd, J=6.0 Hz, 3.2 Hz, 1H), 6.76 (d, J=8.4 Hz, 2H), 6.30-6.27 (m, 4H), 6.04 (s, 1H), 3.32 (q, J=7.2 Hz, 8H), 2.81 (s, 3H), 2.58 (s, 3H), 1.59 (s, 3H), 1.38 (s, 3H), 1.15 (t, J=7.2 Hz, 12H). ^{13}C NMR (100 MHz, $CDCl_3$) δ: 170.92, 157.99, 156.58, 155.55, 152.94, 151.74, 148.14, 144.95, 142.49, 141.94, 135.05, 134.71, 131.96, 130.36, 129.24, 129.16, 127.92, 127.70, 127.12, 123.93, 122.48, 122.09, 110.58, 108.17, 97.38, 62.68, 44.34, 14.81, 14.64, 14.09, 12.88, 12.64. MS (MALDI-TOF): m/z: Calcd. for $C_{48}H_{49}BF_2N_6OS$: 807.375 $[M+H]^+$, Found: 807.451 $[M+H]^+$

3. Cell Imaging

Human A549 lung adenocarcinoma cell lines were grown in DMEM supplemented with 10% FBS (fetal bovine serum) in an atmosphere of 5 % CO_2 at 37 ^{o}C. The cells were plated on 12mm cover glasses in 6-well plate and allowed to grow for 24h. Before the experiments, the cells were washed with PBS buffer, and then the cells were incubated **RhS-BOD** (5 μM) for 40 min at 37 ^{o}C then washed with PBS three times. After incubating with Au^{3+} (5 μM) or Hg^{2+} (5 μM) for 20 min at 37 ^{o}C, cells were rinsed with PBS three times, and DAPI for 15

min at 37 ^{o}C then washed with PBS three times. Then the fluorescence images were acquired through an Olympus CKX41 fluorescence microscope.

References

1. Z. Ekmekci, M. D. Yilmaz and E. U. Akkaya, *Org. Lett.* 2008, **10**, 461.

2. V. Dujolsi, F. Ford and A. W. Czarnik, *J. Am. Chem. Soc.* 1997, **119**, 7386.

3. M. Emrullahoğlu, M. Üçüncü and E. Karakus, *Chem. Commun.*, 2013, **49**, 7836.

4. Absorption and Emission Spectra of RhS-BOD with Hg^{2+}

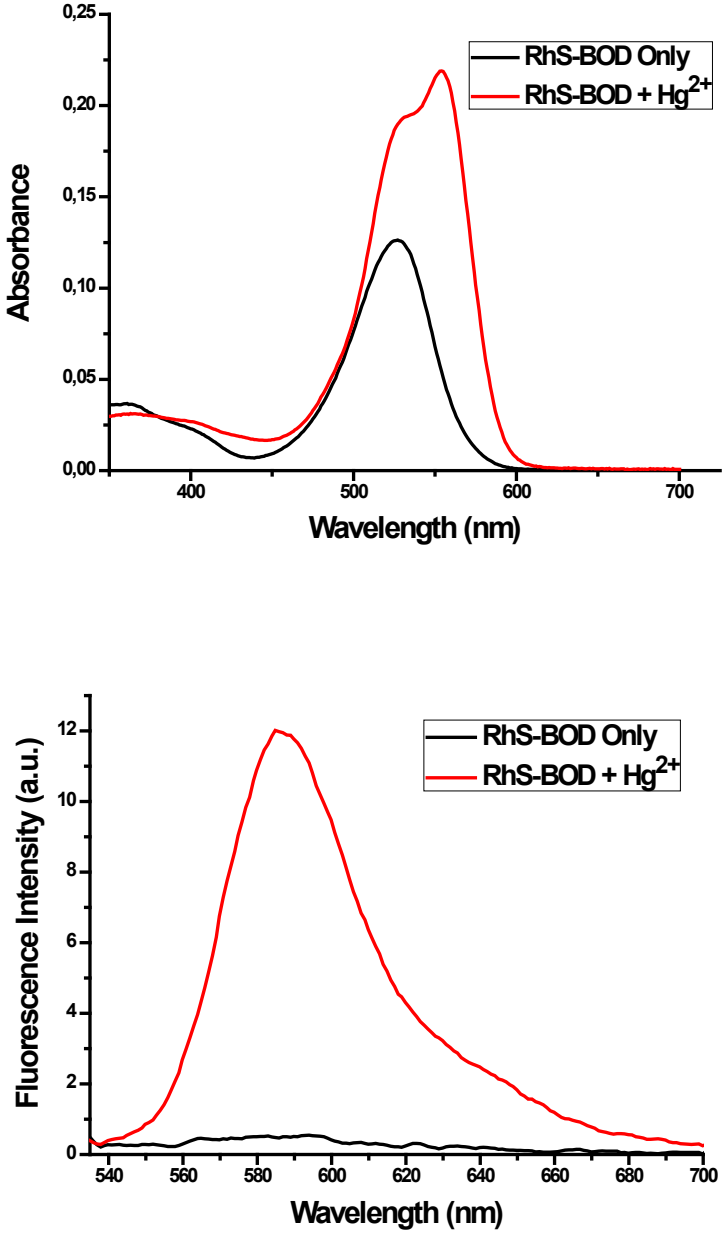

Figure S1 Absorption and Emission spectra of **RhS-BOD** (5 μM) and Hg^{2+} (1.0 equiv.) in 1:1 CH_3CN/HEPES buffer at pH = 7.0; (λ_{ex}: 525 nm).

5. Time-dependent Fluorescence Change of RhS-BOD with Hg^{2+}

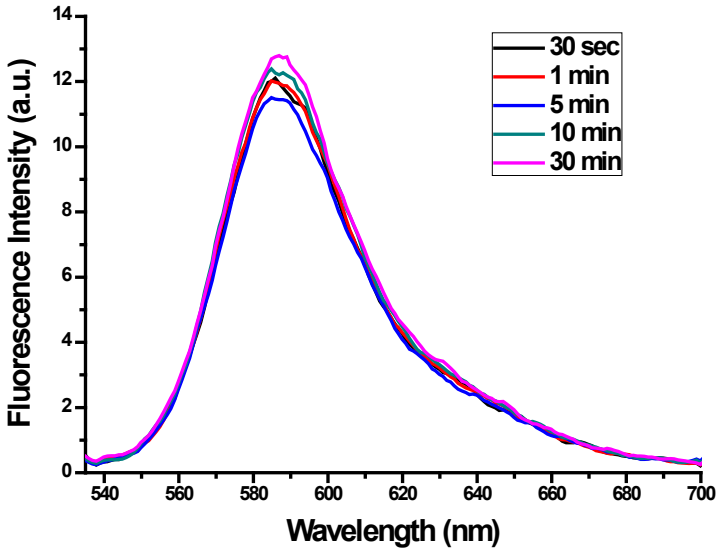

Figure S2 Time-dependent fluorescence change of **RhS-BOD** (5 μM) in the presence of an 1.0 equivalent of $HgCl_2$ measured in 1:1 CH_3CN/HEPES buffer at pH = 7.0

6. Fluorescence Titration of RhS-BOD with Hg^{2+}

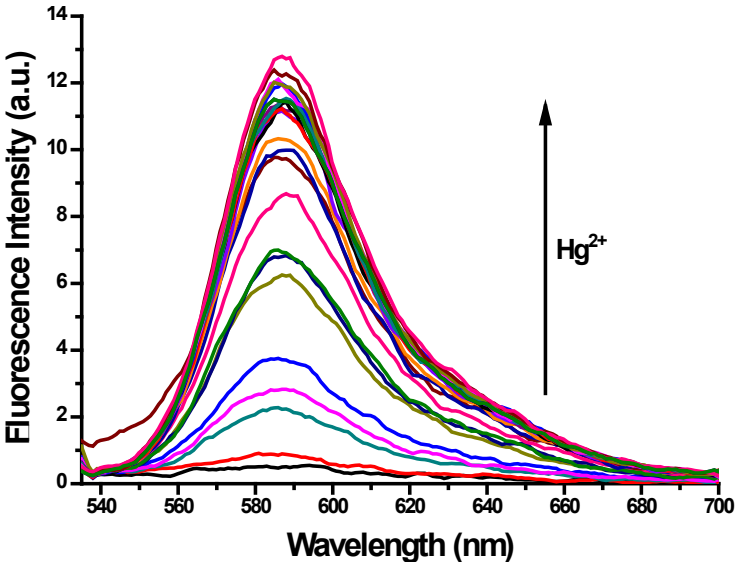

Figure S3 Fluorescence spectra of **RhS-BOD** (5 μM) in 1:1 CH_3CN/HEPES buffer at pH = 7.0 in the presence of Hg^{2+} (mole equivalents = 0.01 - 5.0)

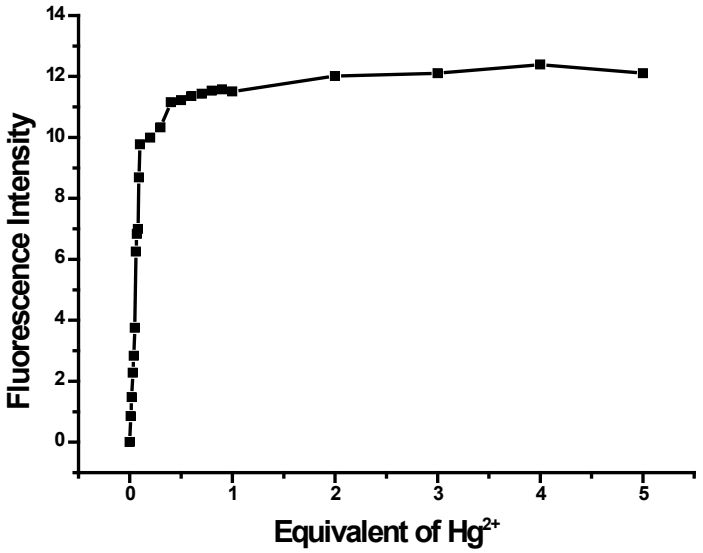

Figure S4 Fluorescence intensity changes of **RhS-BOD** (λ_{max}: 585 nm) vs equivalents of Hg^{2+}

7. The Fluorescence Responses of RhS-BOD with Hg^{2+} and Other Metals

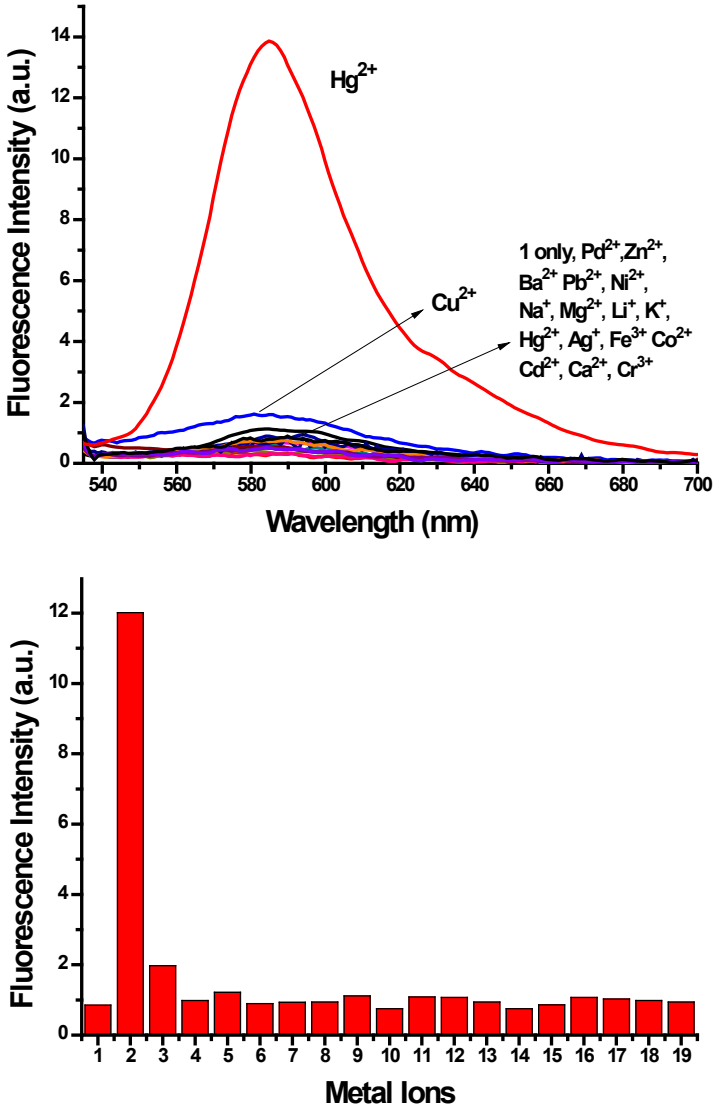

Figure S5 Fluorescence intensities of **RhS-BOD** (5 μM) in 1:1 CH_3CN/HEPES buffer at pH = 7.0 at λ_{max}: 585 nm in the presence of 10.0 equivalent of the cations interest: 1, **RhS-BOD** only; 2, Hg^{2+} (1.0 equiv.); 3, Cu^{2+}; 4, Ag^{+}; 5, Zn^{2+}; 6, Pb^{2+}, 7, Ni^{2+}; 8, Na^{+}; 9, Mg^{2+}; 10, Li^{+}; 11, K^{+}, 12, Pd^{2+}; 13, Fe^{2+}; 14, Co^{2+}; 15, Cd^{2+}; 16, Ca^{2+}; 17, Ba^{2+}; 18, Fe^{3+}; 19, Cr^{3+}

8. The Fluorescence Responses of RhS-BOD in the Presence of Hg^{2+} and Other Metal Ions.

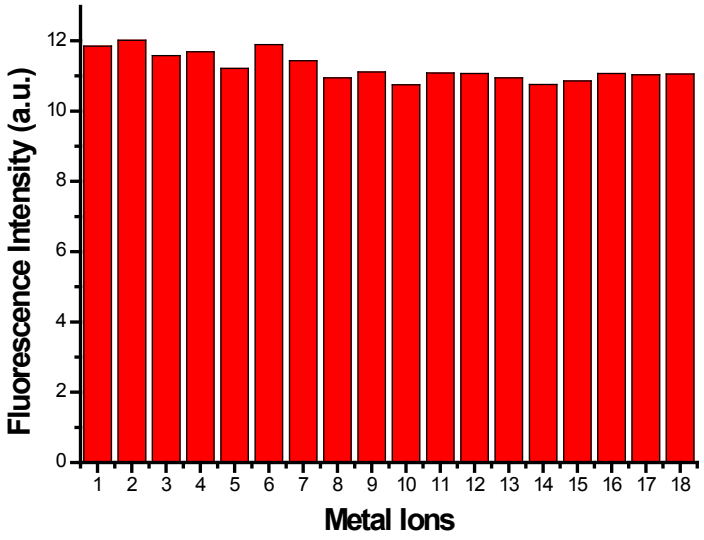

Figure S6 Fluorescence intensities of **RhS-BOD** (5 μM) in 1:1 CH_3CN/HEPES buffer at pH = 7.0 at λ_{max}: 585 nm in the presence Hg^{2+} (1.0 equiv.) and 10.0 equiv the following metal ions: 1, none; 2, Cu^{2+}; 3, Ag^{+}; 4, Zn^{2+}; 5, Pb^{2+}; 6, Ni^{2+}; 7, Na^{+}; 8, Mg^{2+}; 9, Li^{+}; 10, K^{+}, 11, Pd^{2+}; 12, Fe^{2+}; 13, Co^{2+}; 14, Cd^{2+}; 15, Ca^{2+}; 16, Ba^{2+} 17, Cr^{3+}; 18, Fe^{3+}

9. The Fluorescence Intensity Changes of RhS-BOD in the Presence of Hg^{2+} and CN^{-} Ions.

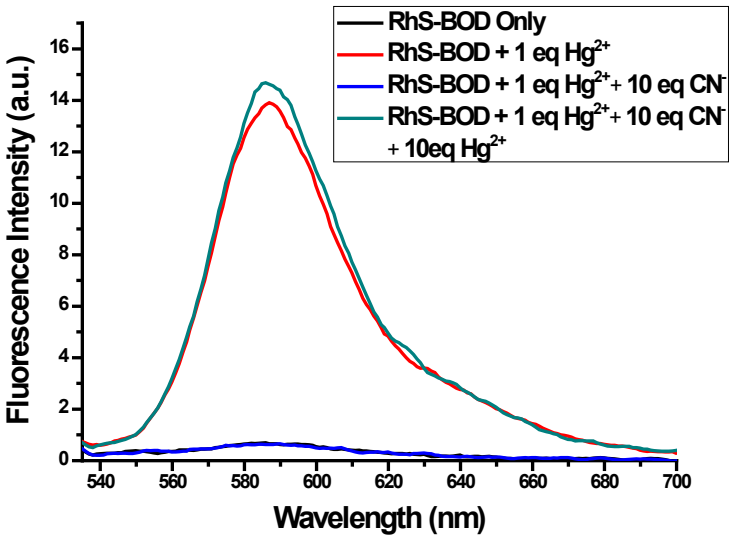

Figure S7 Fluorescence intensity changes of **RhS-BOD** (5 μM) in 1:1 CH_3CN/HEPES buffer at pH = 7.0 at λ_{max}: 585 after addition of 1 equiv. Hg^{2+}, 1 equiv. Hg^{2+} + 10 equiv. CN^{-} and 1 equiv. Hg^{2+} + 10 equiv. CN^{-} + 10 equiv. Hg^{2+} respectively.

10. Effect of pH

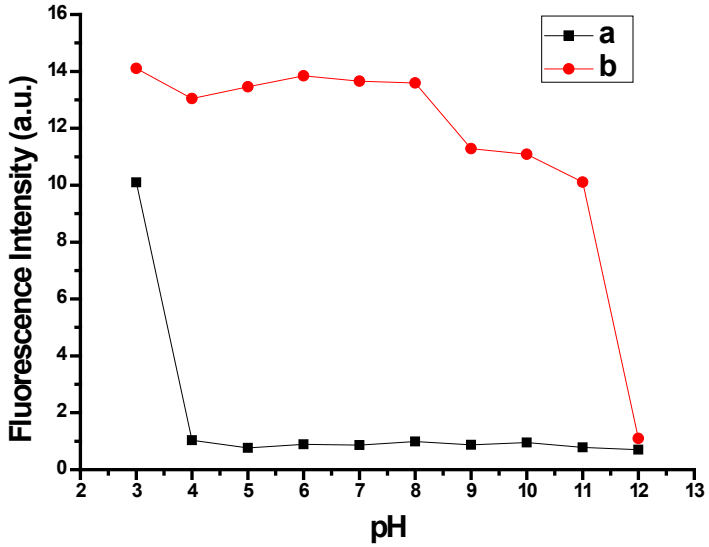

Figure S8 Effect of pH on the fluorescence intensity of **RhS-BOD** (5 μM) in 1:1 CH_3CN/HEPES in the absence **(a)** and presence **(b)** of Hg^{2+} (1.0 equiv.) λ_{max}: 585

11. Job's Plot

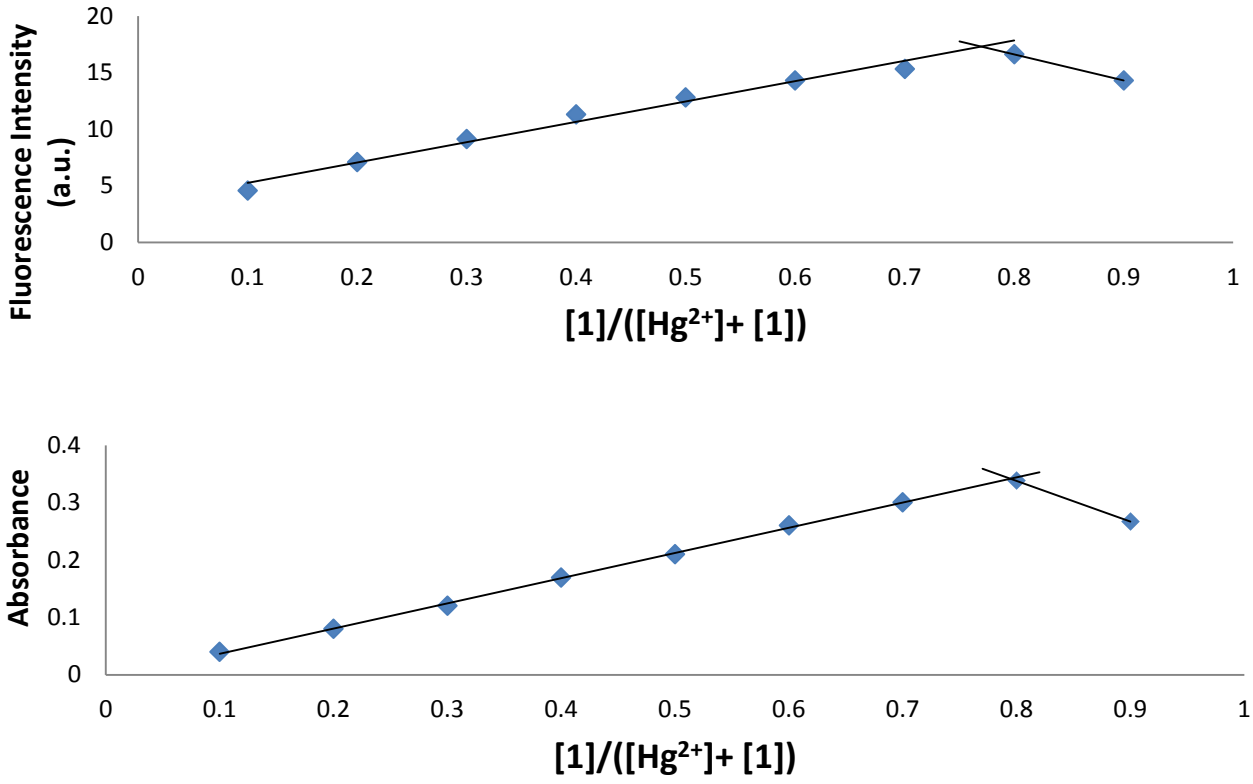

Figure S9 Job's plots for the **RhS-BOD** and Hg^{2+} in 1:1 CH_3CN/HEPES solution

12. Determination of Detection Limit of Hg^{2+}

The detection limit was calculated based on the fluorescence titration. To determine the S/N ratio, the emission intensity of **RhS-BOD** (5 μM) without Hg^{2+} was measured by 10 times and the standard deviation of blank measurements was determined. Under the present conditions, a good linear relationship between the fluorescence intensity and Hg^{2+} concentration could be obtained in the 0 – 0.3 μM (R = 0.9885). The detection limit is then calculated with the equation: detection limit = 3σbi/m, where σbi is the standard deviation of blank measurements; m is the slope between intensity versus sample concentration. The detection limit was measured to be 8 nM at S/N = 3.

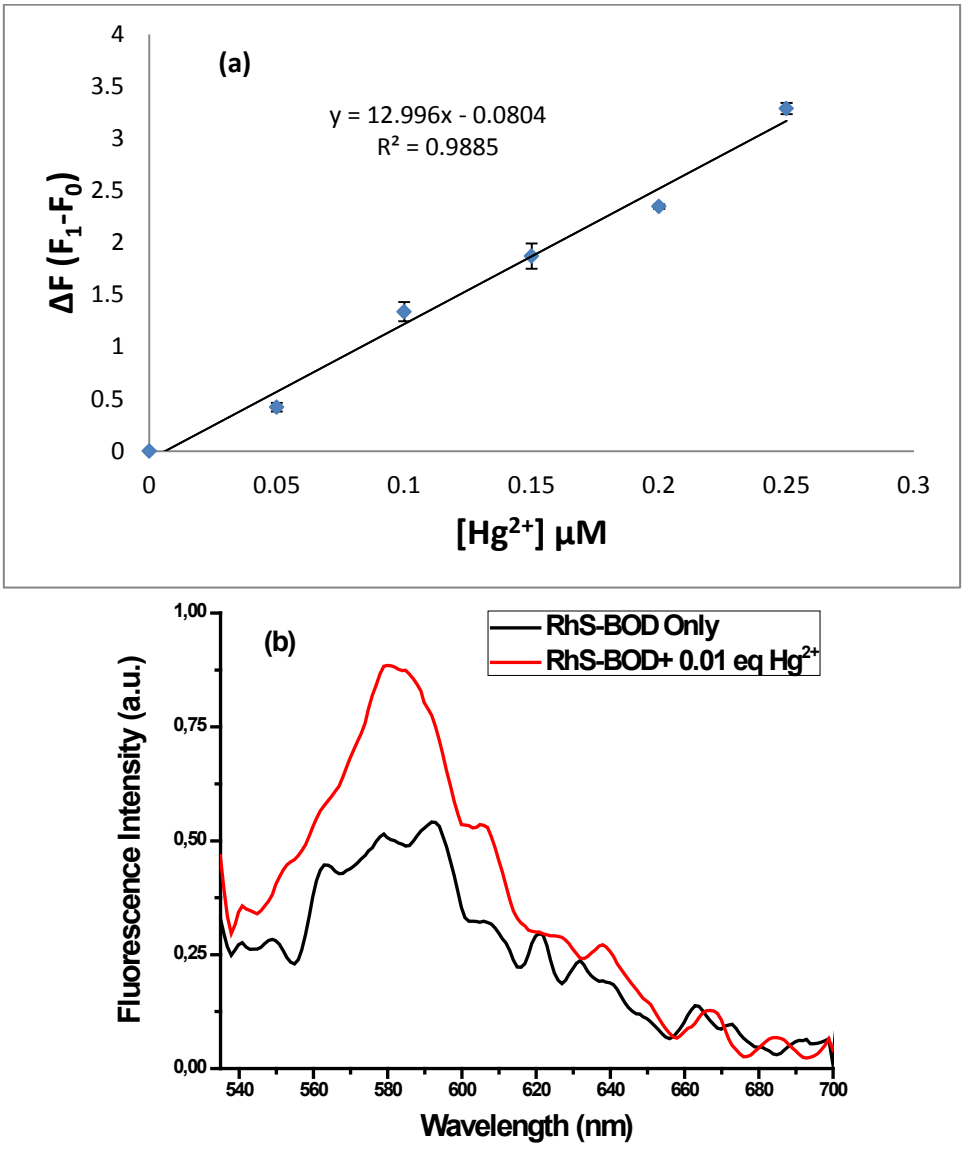

Figure S10 (a) Fluorescence changes of **RhS-BOD** (5.0 μM) upon addition of Hg^{2+} (0.05 to 0.3 μM, 0.01 to 0.05 equiv.) **(b)** Fluorescence spectra of **RhS-BOD** (5.0 μM) in the presence of Hg^{2+} (0.05 μM, 0.01 equiv.) in 1:1 CH_3CN/HEPES buffer at pH = 7.0

13. Absorption and Emission Spectra of RhS-BOD with Au^{3+} at λ_{ex}: 470 nm

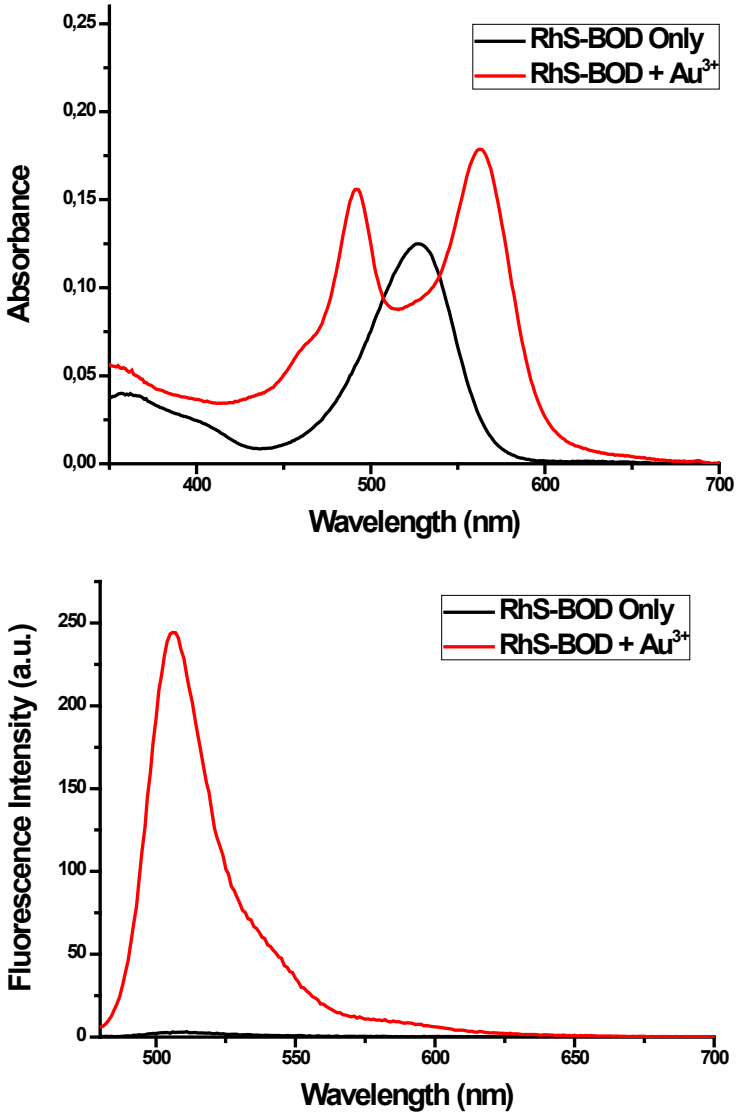

Figure S11 Absorption and Emission spectra of **RhS-BOD** (5 μM) and Au^{3+} (1.0 equiv.) in 1:1 CH_3CN/HEPES buffer at pH = 7.0

14. Time-dependent Fluorescence Change of RhS-BOD with Au^{3+} at λ_{ex}: 470 nm

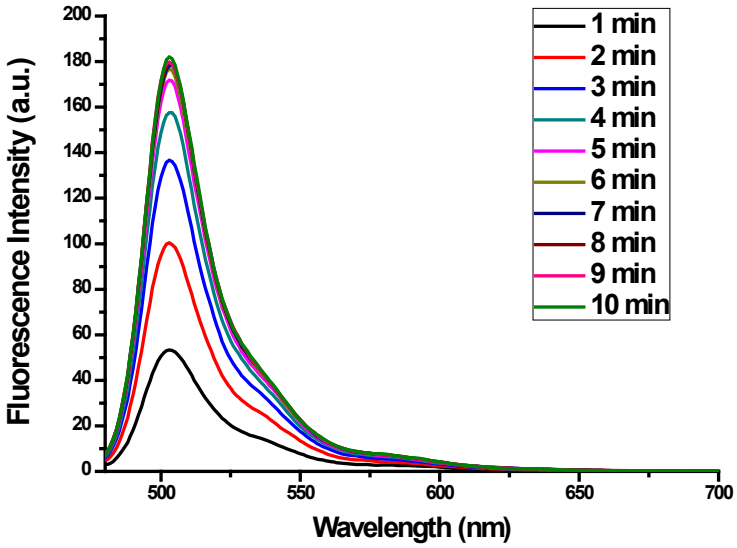

Figure S12 Time-dependent fluorescence change of **RhS-BOD** (5 μM) in the presence of an 1.0 equivalent of $AuCl_3$ measured in 1:1 CH_3CN/HEPES buffer at pH = 7.0

15. Fluorescence Titration of RhS-BOD with Au^{3+} at λ_{ex}: 470 nm and λ_{ex}: 525 nm

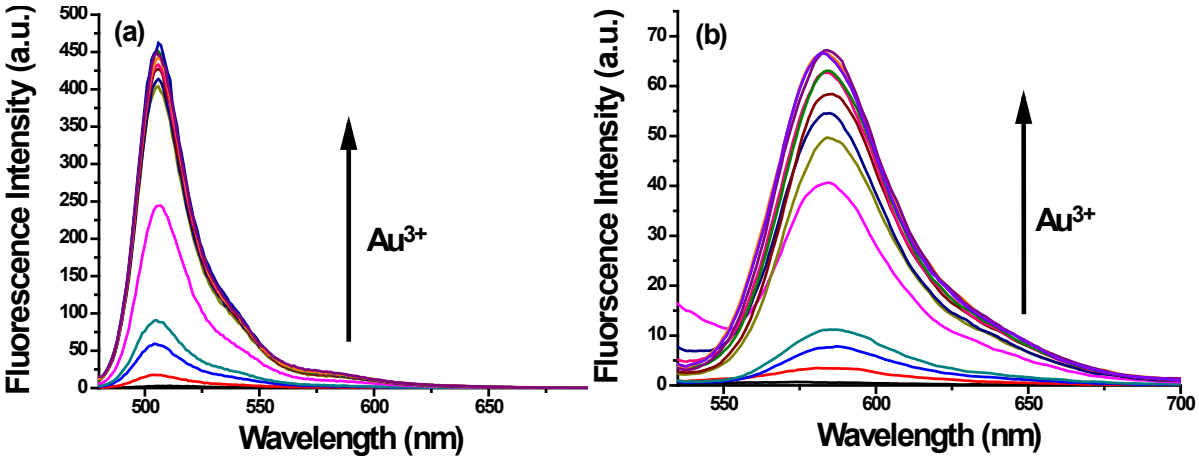

Figure S13 Fluorescence spectra of **RhS-BOD** (5 μM) in 1:1 CH_3CN/HEPES buffer at pH = 7.0 in the presence of Au^{3+} (mole equivalents = 0 - 10.0) **(a)** λ_{ex}**:** 470 nm **(b)** λ_{ex}: 525 nm

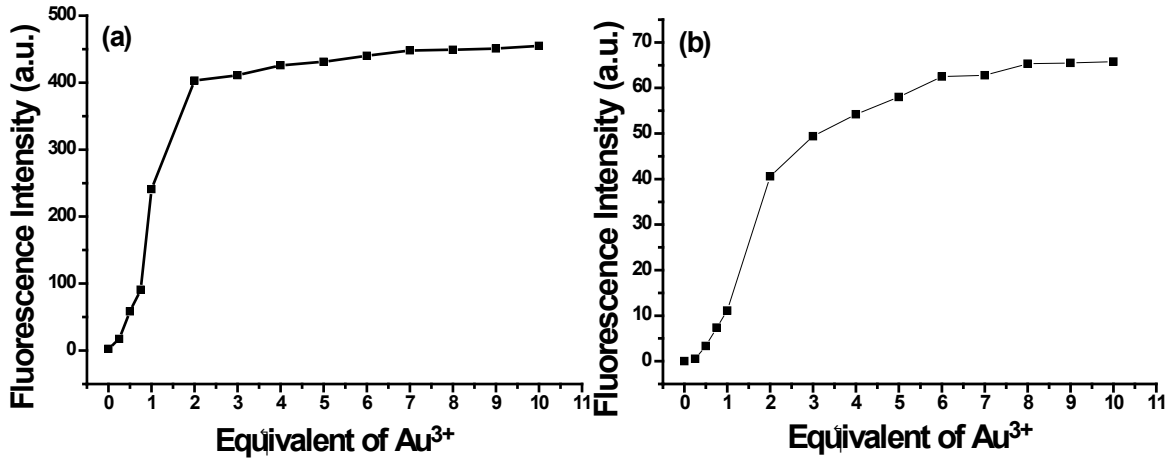

Figure S14 Fluorescence intensity changes of **RhS-BOD** vs equivalents of Au^{3+} **(a)** λ_{ex}**:** 470 nm **(b)** λ_{ex}: 525 nm

16. The Fluorescence Responses of RhS-BOD with Au^{3+} and Other Metals at λ_{ex}: 470 nm

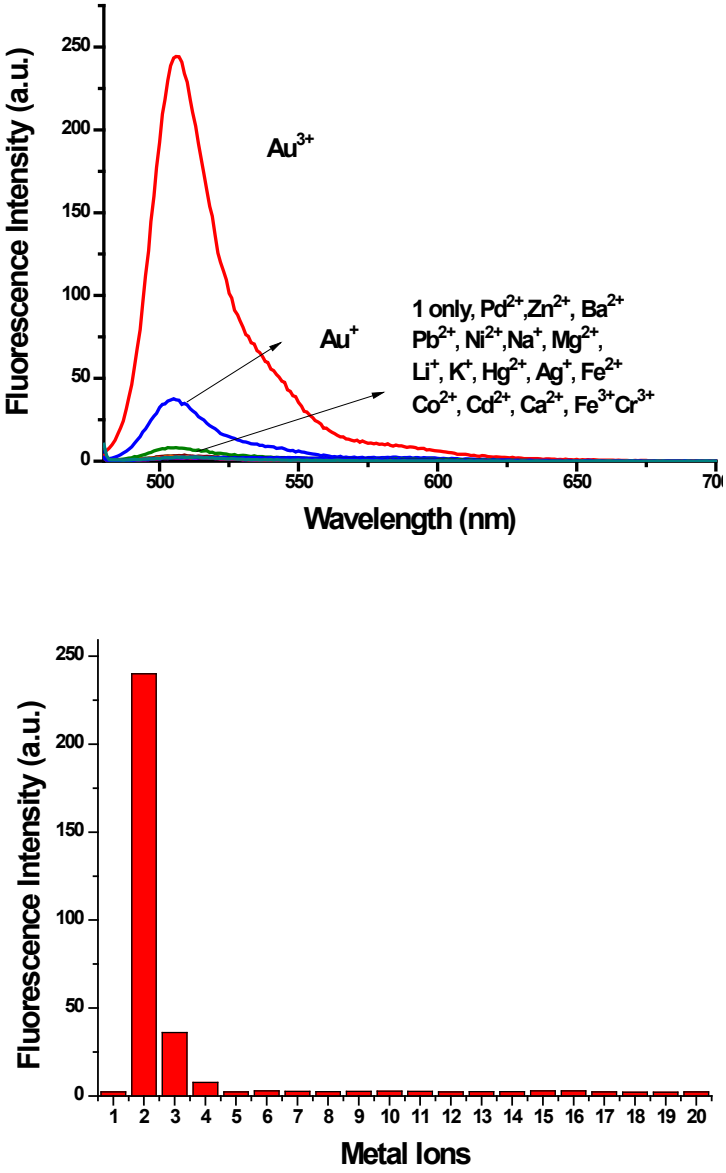

Figure S15 Fluorescence intensities of **RhS-BOD** (5 μM) in 1:1 CH_3CN/HEPES buffer at pH = 7.0 at λ_{max}: 506 nm in the presence of 10.0 equivalent of the cations interest: 1, **RhS-BOD** only; 2, Au^{3+} (1.0 equiv.); 3, Au^{+}; 4, Cu^{2+}; 5, Zn^{2+}; 6, Pb^{2+}, 7, Ni^{2+}; 8, Na^{+}; 9, Mg^{2+}; 10, Li^{+}; 11, K^{+}, 12, Pd^{2+}; 13, Fe^{2+}; 14, Co^{2+}; 15, Cd^{2+}; 16, Ca^{2+}; 17, Ba^{2+}; 18, Ag^{+} 19, Fe^{3+}; 20, Cr^{3+}

17. The Fluorescence Responses of RhS-BOD in the Presence of Au^{3+} and Other Metal Ions at λ_{ex}: 470 nm

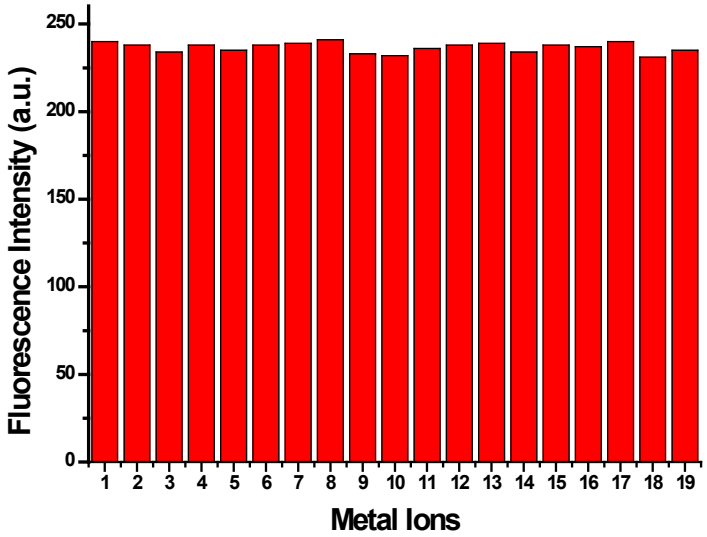

Figure S16 Fluorescence intensities of **RhS-BOD** (5 μM) in 1:1 CH_3CN/HEPES buffer at pH = 7.0 at λ_{max}: 506 nm in the presence Au^{3+} (1.0 equiv.) and 10.0 equiv the following metal ions: 1, none; 2, Au^{+}; 3, Cu^{2+}; 4, Zn^{2+}; 5, Pb^{2+}; 6, Ni^{2+}; 7, Na^{+}; 8, Mg^{2+}; 9, Li^{+}; 10, K^{+}, 11, Pd^{2+}; 12, Fe^{2+}; 13, Co^{2+}; 14, Cd^{2+}; 15, Ca^{2+}; 16, Ba^{2+} 17, Ag^{+}; 18, Cr^{3+}; 19, Fe^{3+}

18. Effect of pH at λ_{ex}: 470 nm

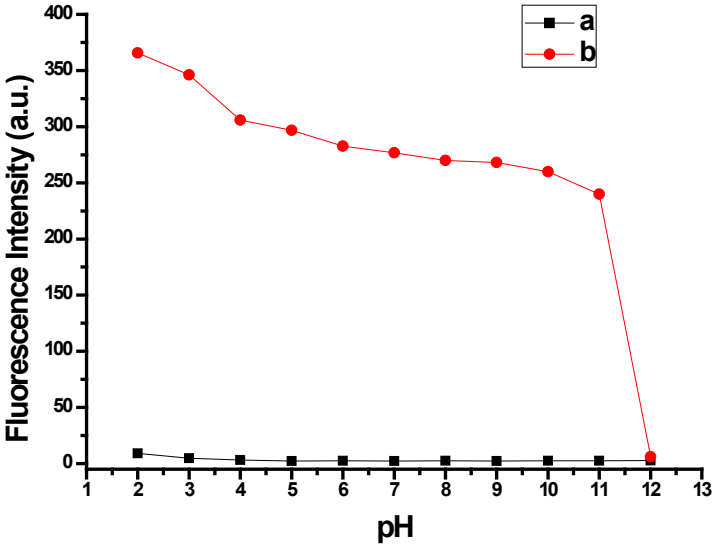

Figure S17 Effect of pH on the fluorescence intensity of **RhS-BOD** (5 μM) in 1:1 CH_3CN/HEPES in the absence **(a)** and presence **(b)** of Au^{3+} (1.0 equiv.) λ_{max}: 506 nm

19. Determination of Detection Limit of Au^{3+} at λ_{ex}: 470 nm

The detection limit was calculated based on procedure mentioned before and the detection limit was measured to be 65 nM at S/N = 3.

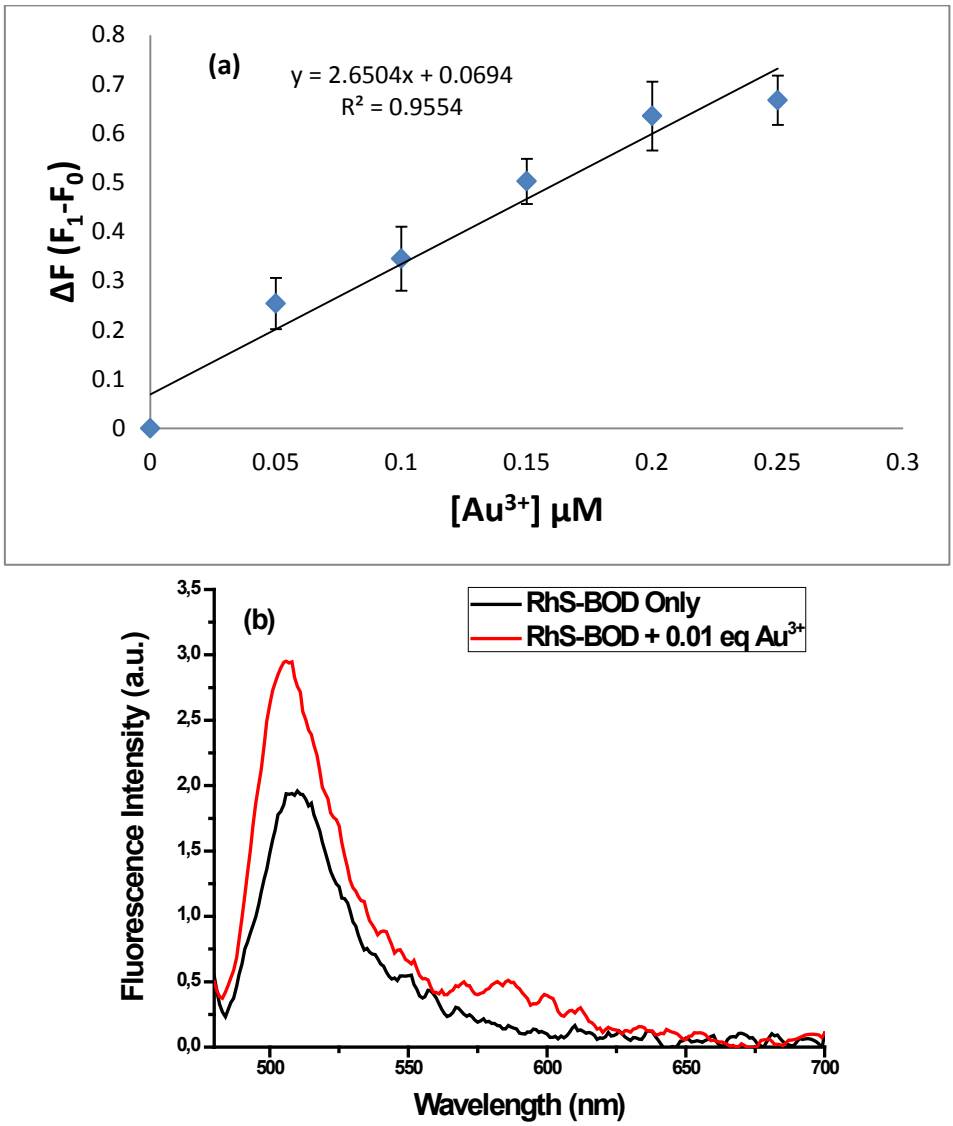

Figure S18 (a) Fluorescence changes of **RhS-BOD** (5.0 µM) upon addition of Au^{3+} (0.05 to 0.3 µM, 0.01 to 0.05 equiv.) **(b)** Fluorescence spectra of **RhS-BOD** (5.0 µM) in the presence of Au^{3+} (0.05 µM, 0.01 equiv.) in 1:1 CH_3CN/HEPES buffer at pH = 7.0

20. Determination of detection Limit of Au^{3+} at λ_{ex}: 525 nm

The detection limit was calculated based on procedure mentioned before and the detection limit was measured to be 10 nM at S/N = 3.

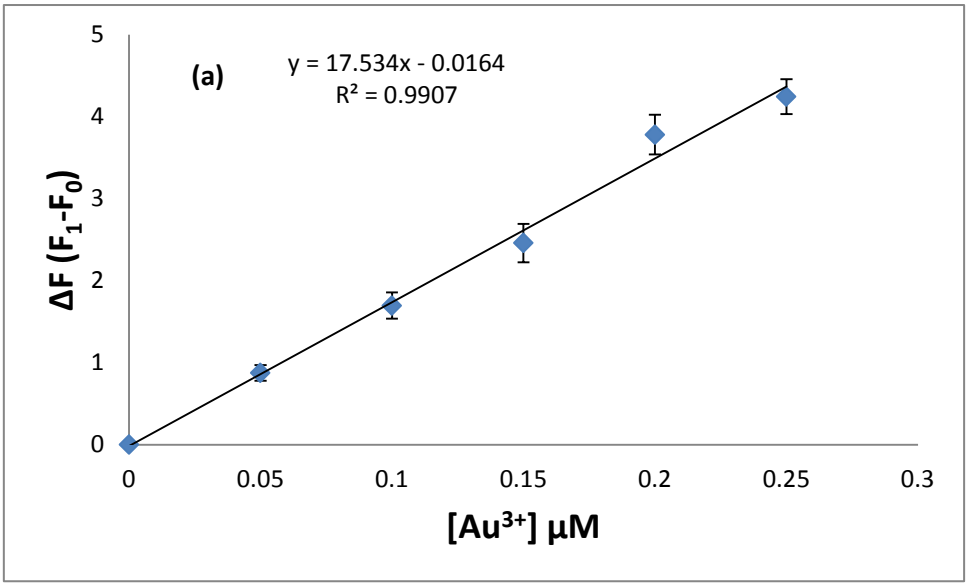

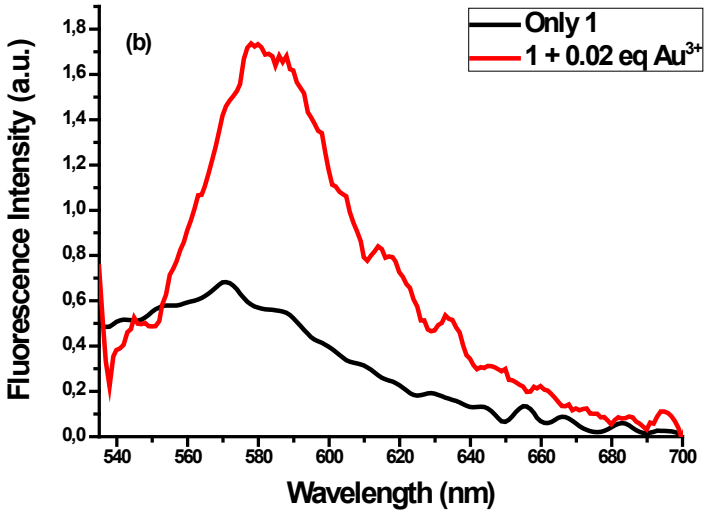

Figure S19(a) Fluorescence changes of **RhS-BOD** (5.0 µM) upon addition of Au^{3+} (0.05 to 0.3 µM, 0.01 to 0.05 equiv.) at λ_{ex}: 525 nm **(b)** Fluorescence spectra of **RhS-BOD** (5.0 µM) in the presence of Au^{3+} (0.05 µM, 0.01 equiv.) in 1:1 CH_3CN/HEPES buffer at pH = 7.0

21. Job's Plot for Au^{3+} at λ_{ex}: 525 nm

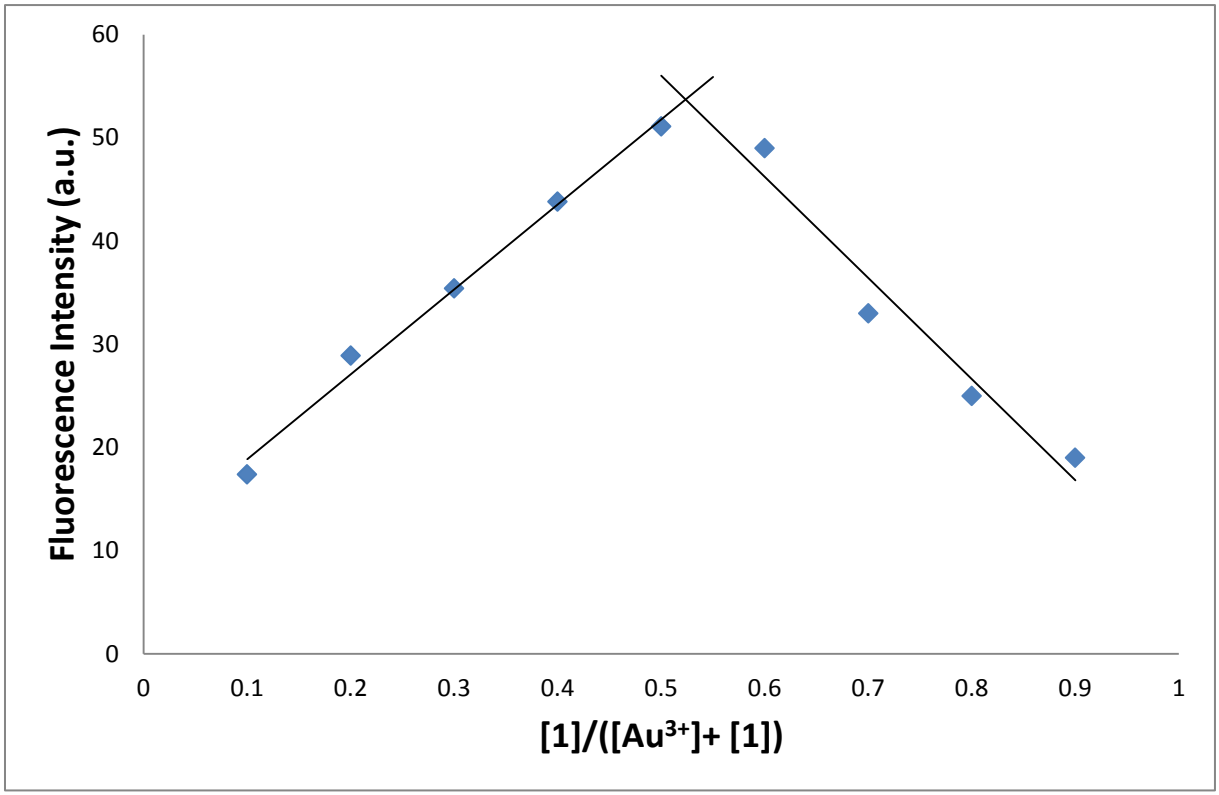

Figure S20 Job's plot for the **RhS-BOD** and Au^{3+} in 1:1 CH_3CN/HEPES solution at λ_{ex}: 525 nm

^{1}H NMR of RhO-BOD

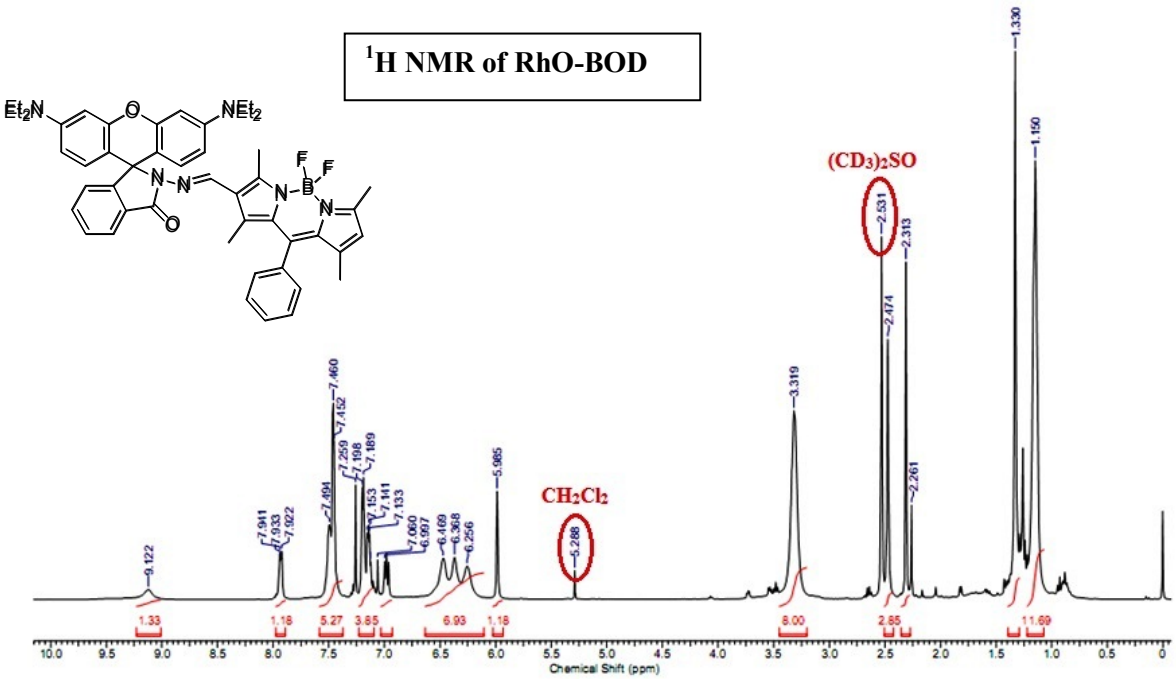

^{13}C NMR of RhO-BOD

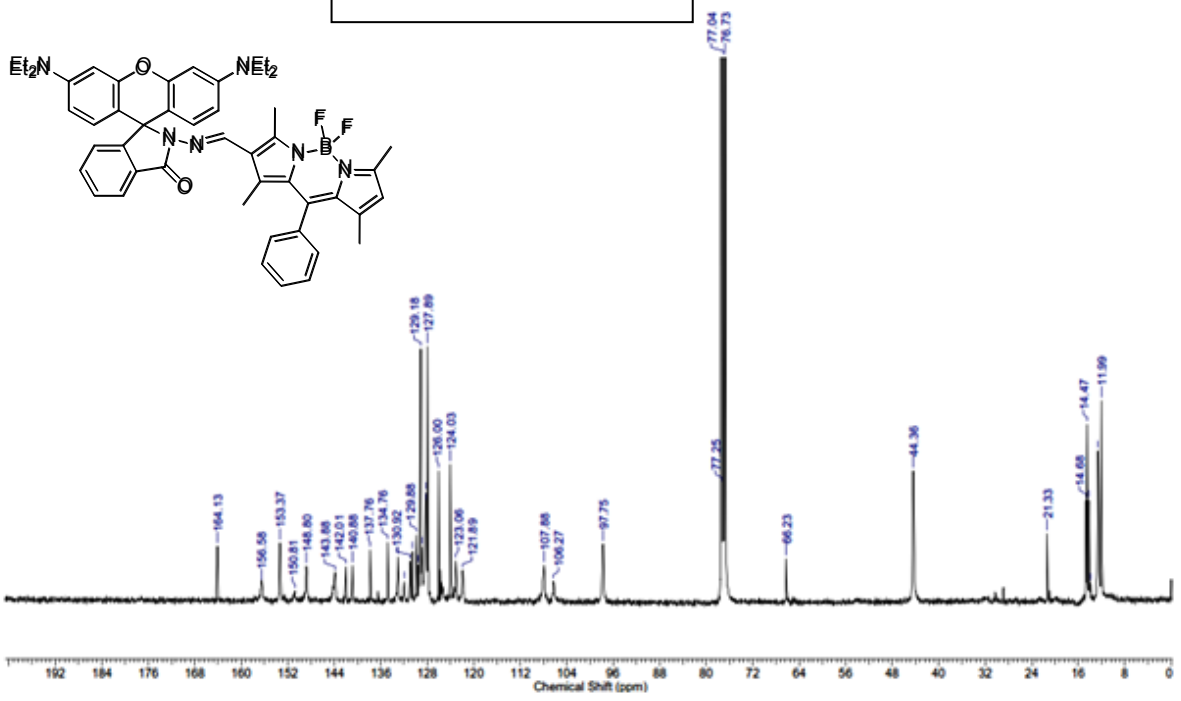

^{1}H NMR of RhS-BOD

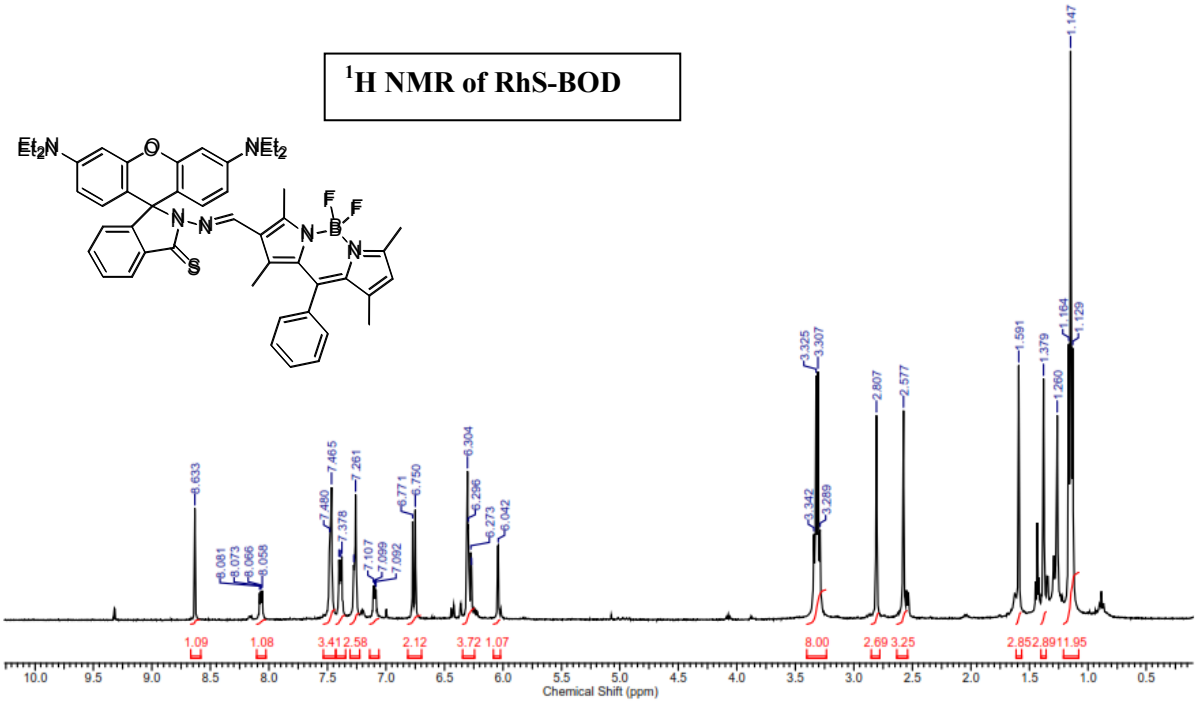

^{13}C NMR of RhS-BOD

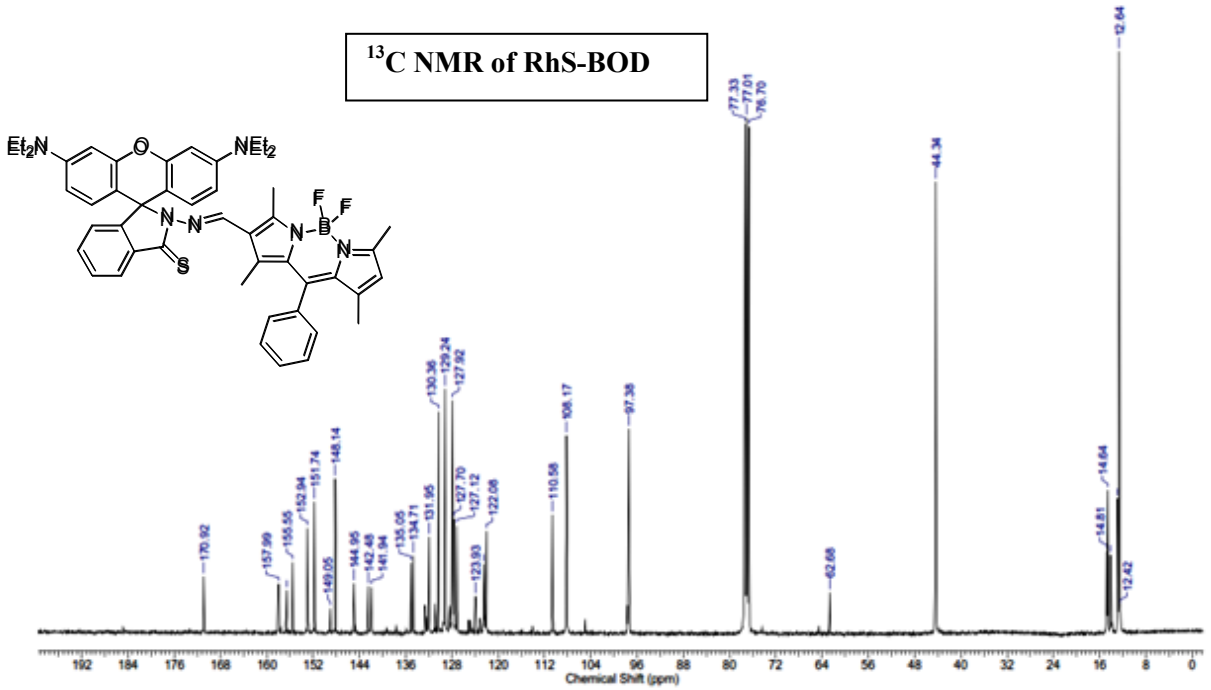

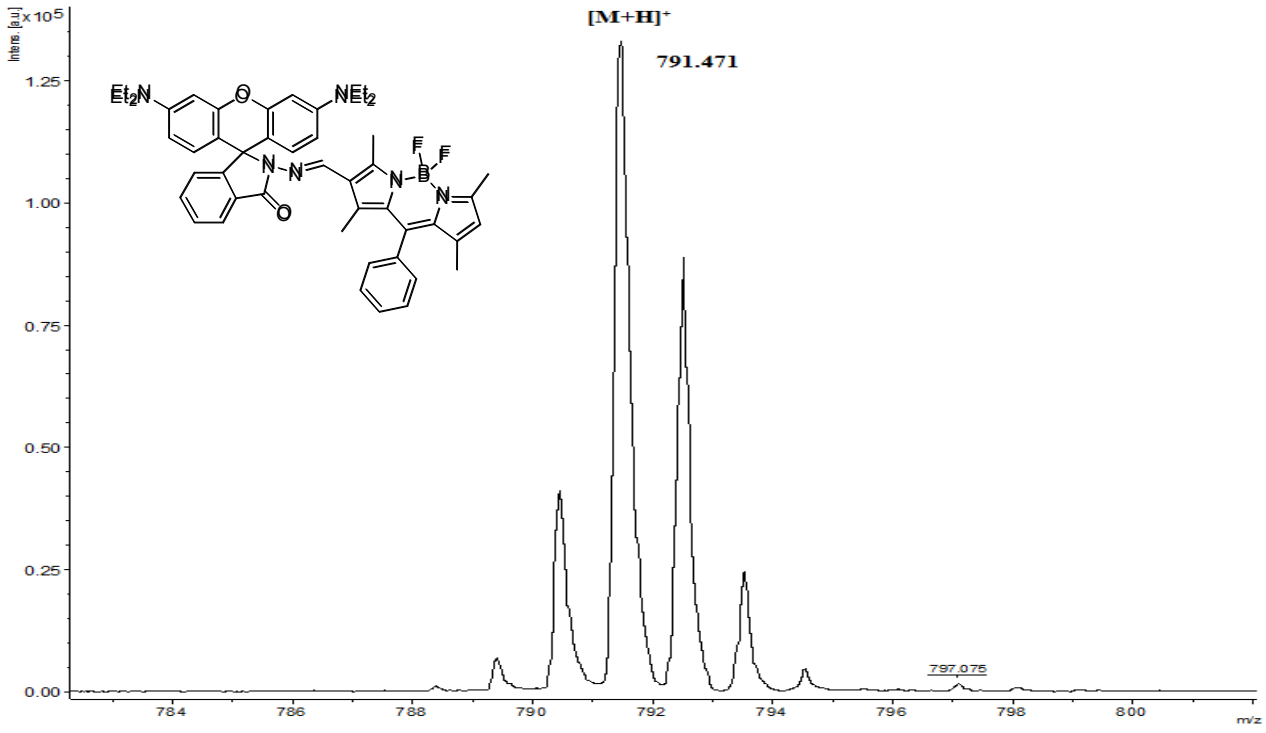

MALDI-TOF result of **RhO-BOD**

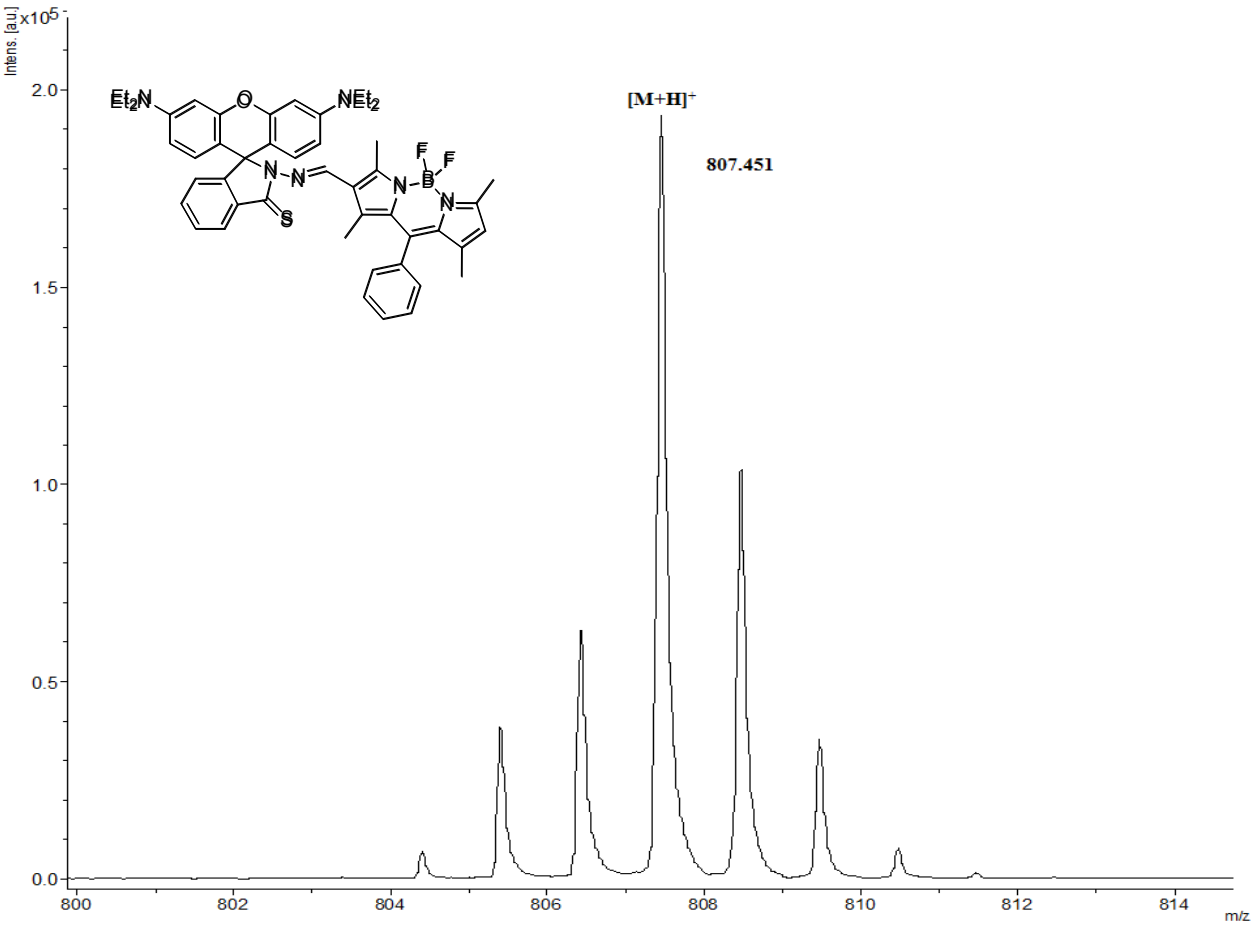

MALDI-TOF result of **RhS-BOD**

22. TLC Image of the Hydrolysis Reaction of RhS-BOD Mediated by Au(III) Ions

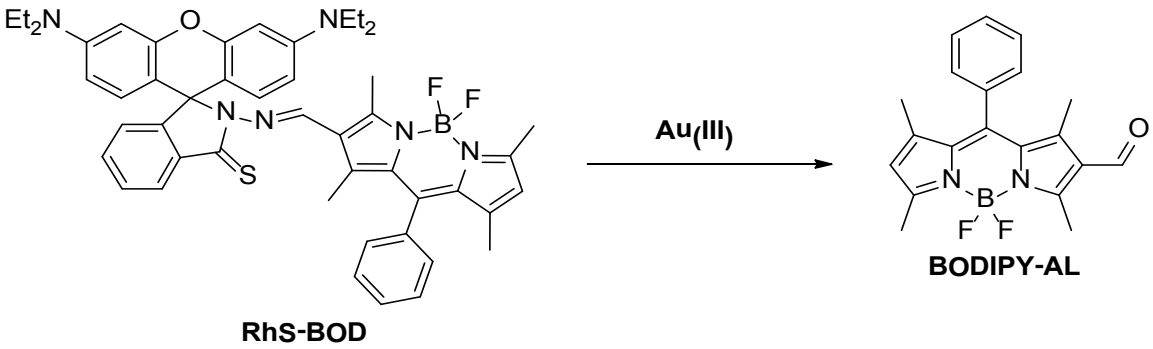

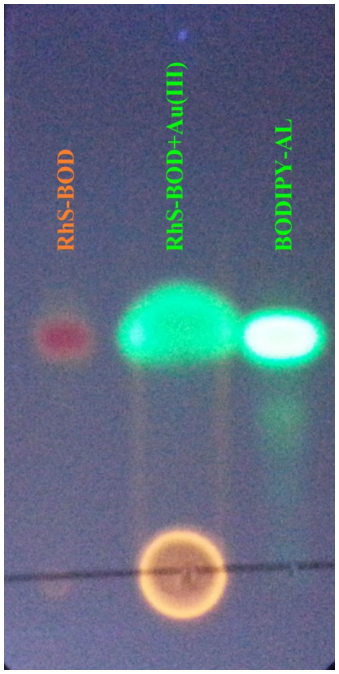

Figure S21 TLC image of the hydrolysis reaction of **RhS-BOD** mediated with Au (III) ion

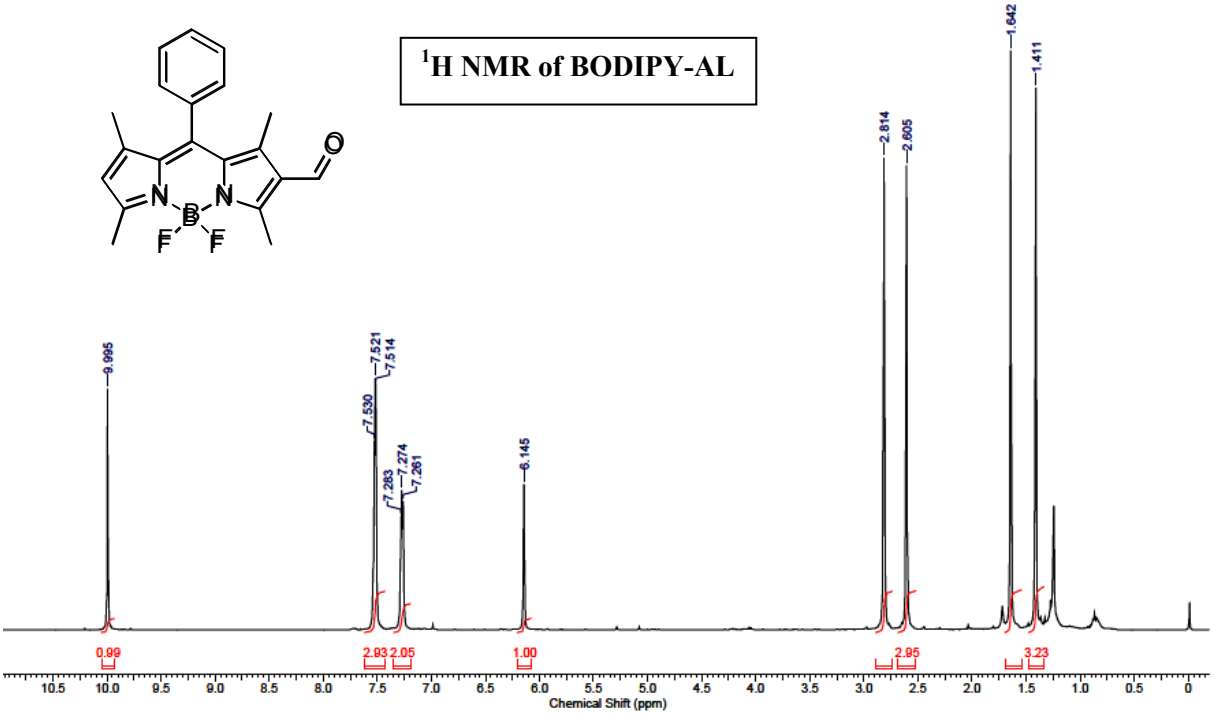
^{1}H NMR of BODIPY-AL
9.995
7.521
7.514
7.530
7.283
7.274
7.261
6.145
2.814
2.805
1.642
1.411
0.99
2.93
2.05
1.00
2.95
3.23
Chemical Shift (ppm)

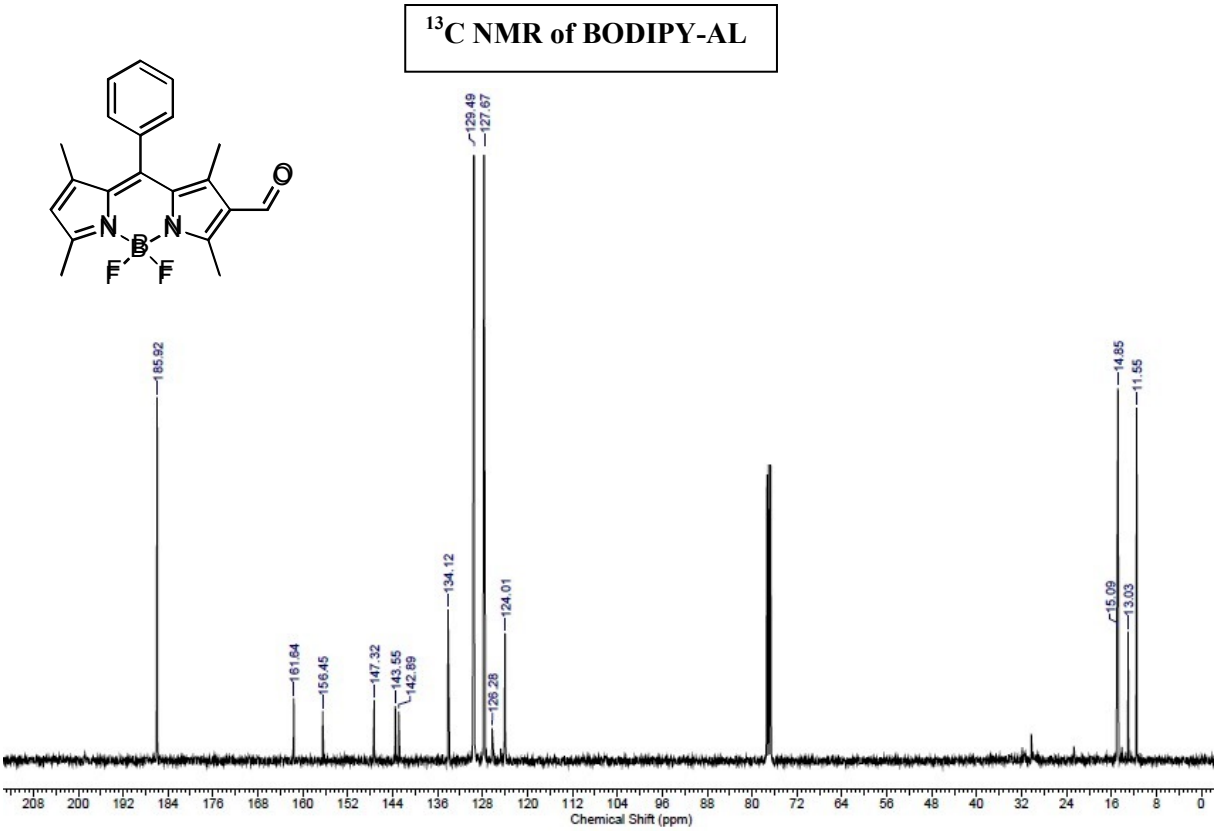
^{13}C NMR of BODIPY-AL
185.92
161.64
156.45
147.32
143.55
142.89
134.12
129.49
127.67
126.28
124.01
15.09
14.85
13.03
11.55
Chemical Shift (ppm)